nature geoscience
SUPPLEMENTARY INFORMATION
DOI: 10.1038/NGEO2370

High Poisson's ratio of Earth's inner core explained by carbon alloying

C. Prescher[1,2], L. Dubrovinsky[1], E. Bykova[1], I. Kupenko[1,3], K. Glazyrin[1], A. Kantor[1,3], C. McCammon[1], M. Mookherjee[1,4], Y. Nakajima[1,5], N. Miyajima[1], R. Sinmyo[1], V. Cerantola[1], N. Dubrovinskaia[6], V. Prakapenka[2], R. Rüffer[3], A. Chumakov[3,7] & M. Hanfland[3]

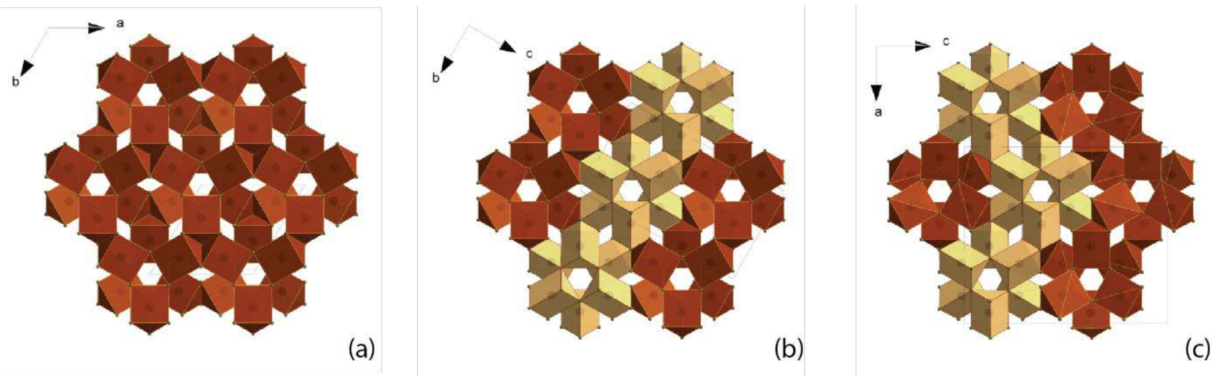

Figure S1 | Crystal structures of known Fe_7C_3 polytypes as polyhedral models. The building units are CFe_6 prisms, where each 3 prisms are connected via shared vertices in triads and stacked with 60° rotation relative to their upper and lower neighbors in columns. The columns may be oriented upwards (light brown) or downwards (dark brown) and they are connected to each other by common edges. Different ways of column packing produce different Fe_7C_3 polytypes: hexagonal $P6_3mc$ (*a*), orthorhombic *Pnma* (*b*) and orthorhombic *Pbca* (*c*) structures. For the sake of comparison 3 similar units are depicted in an identical orientation, and thin solid lines designate unit cell edges.

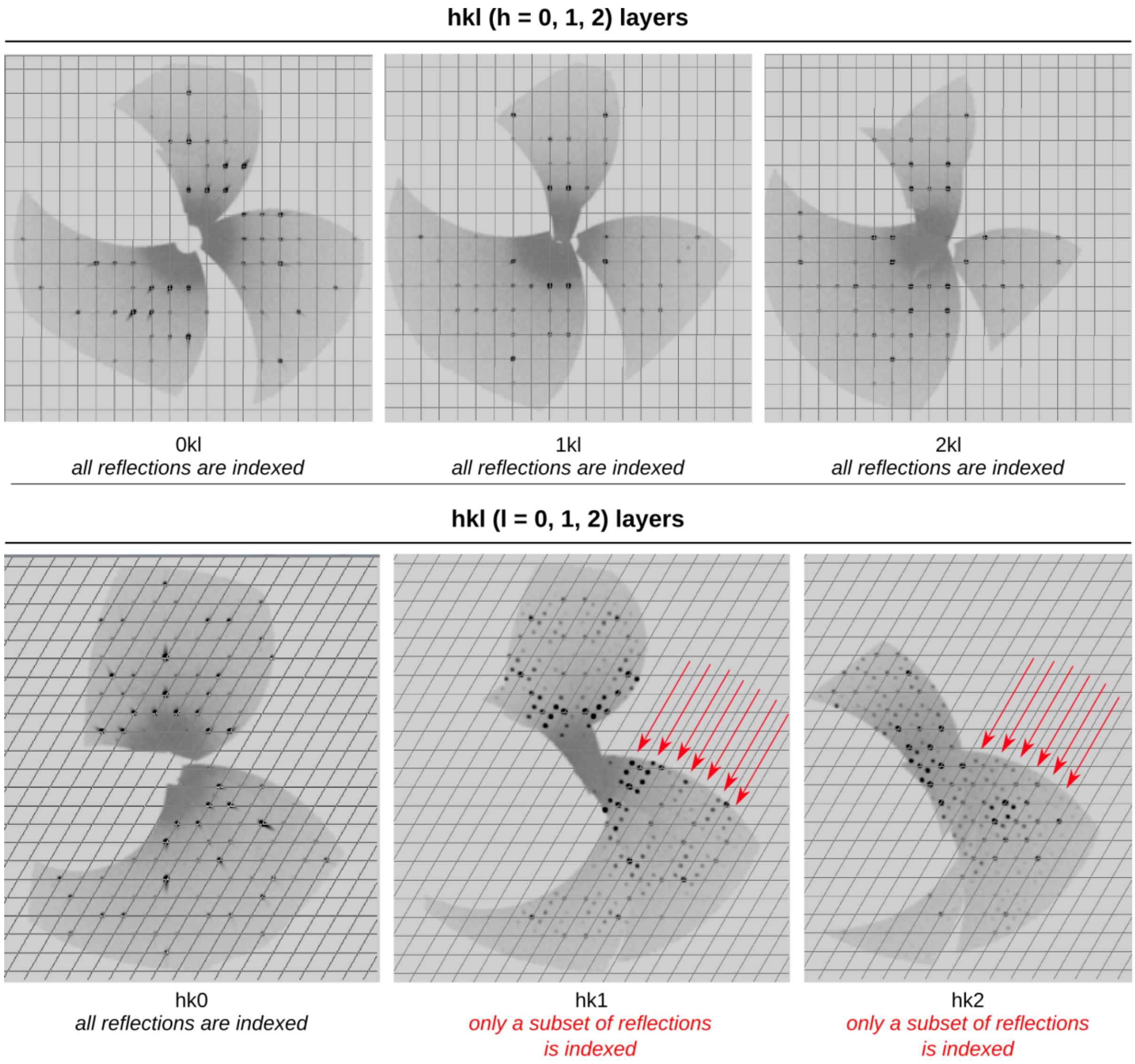

Fig S2. Reciprocal lattice reconstruction for experimentally observed o-Fe_7C_3 reflections when considered in a hexagonal unit cell. The images show several lattice reconstructions of different *hkl* planes in the $P6_3mc$ space group. The grid in each image represents the reciprocal lattice of $P6_3mc$ and the dots are the actual reflections of o-Fe_7C_3. For some crystallographic orientations of o-Fe_7C_3, observed reflections may be described within a hexagonal space group, while other reflections (red arrows) can be described only within the orthorhombic *Pbca* space group. If the dataset is limited or some reflections are omitted for whatever reason, the symmetry of o-Fe_7C_3 may be wrongly assigned as hexagonal.

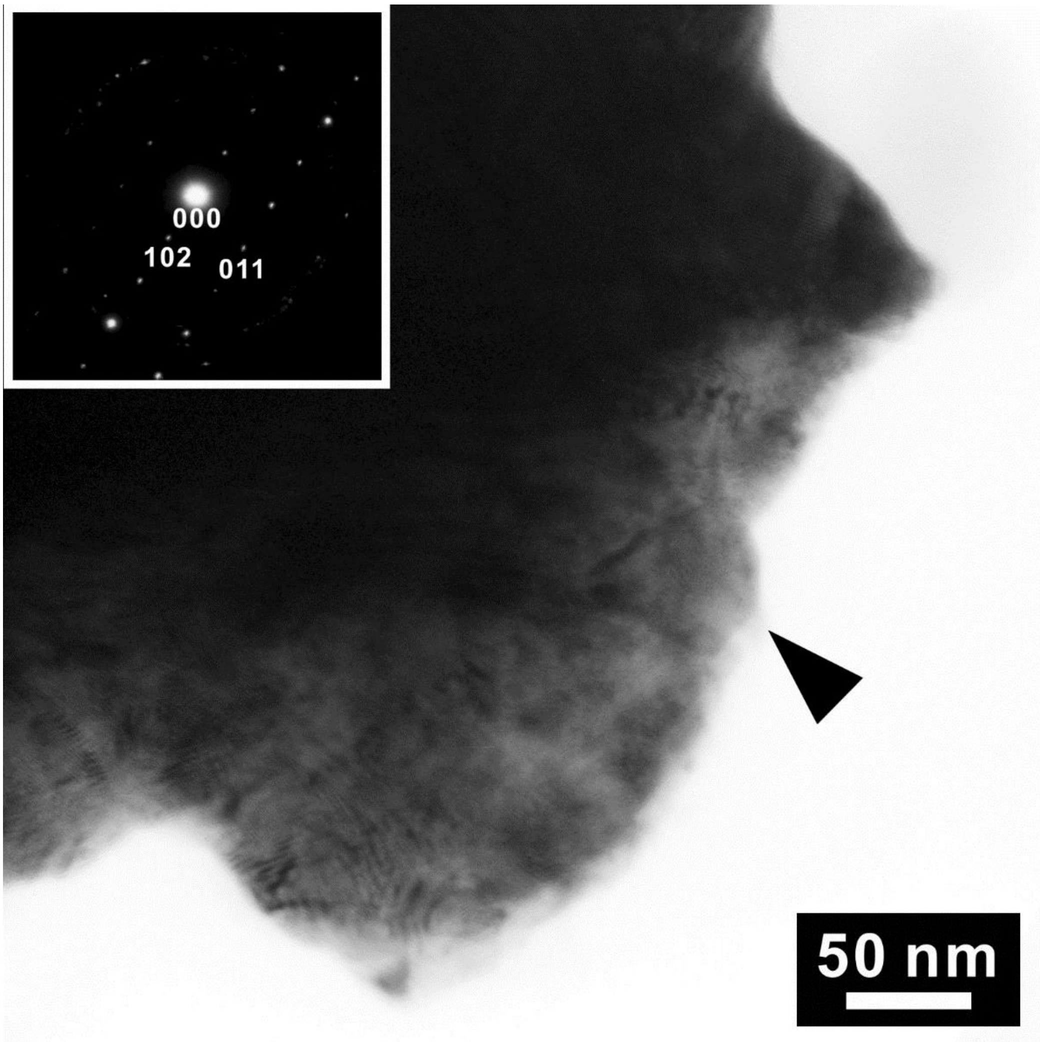

Figure S3 | Bright field transmission electron microscopy image of o-Fe_7C_3 recovered after melting in a laser heated diamond anvil cell at 180 GPa and about 4000 K. The selected area diffraction pattern (upper-left inset) of the centre grain indicated by the triangle arrow is indexed with a unit cell of a= 11.65 Å, b = 4.35 Å, c= 13.43 Å and a zone axis of [$\bar{2}$ $\bar{1}$ 1].

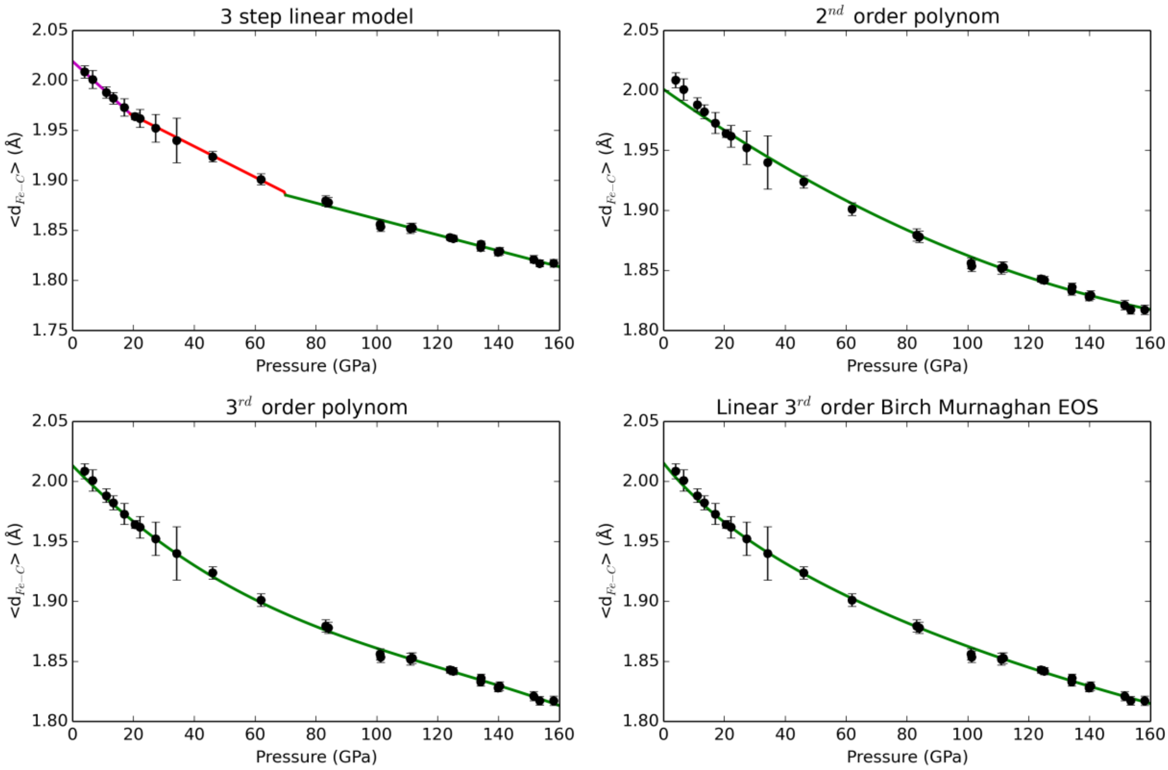

Figure S4. Comparison of fits to the variation of mean Fe-C distance versus pressure weighted according to the error bars. Systematic misfits demonstrate that neither 2nd nor 3rd order polynomials nor a 3rd order Birch Murnaghan equation of state provides an accurate model of the data. The three-step linear model is therefore preferred. Changes in slope coincide with electronic transitions in Fe_7C_3.

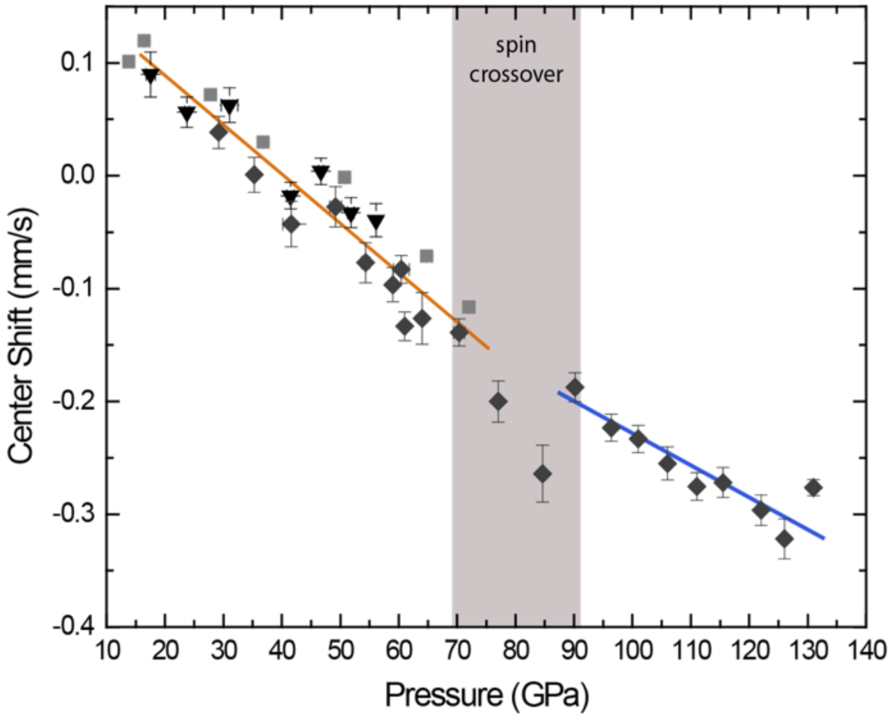

Figure S5 | Pressure effect on the mean center shift of Fe_7C_3 quadrupole doublets. Different experiments are indicated by different symbols. The data show two linear pressure trends with a change in slope between regions. The transition marks a change in the electronic configuration of Fe_7C_3 which can be related to a paramagnetic to nonmagnetic transition.

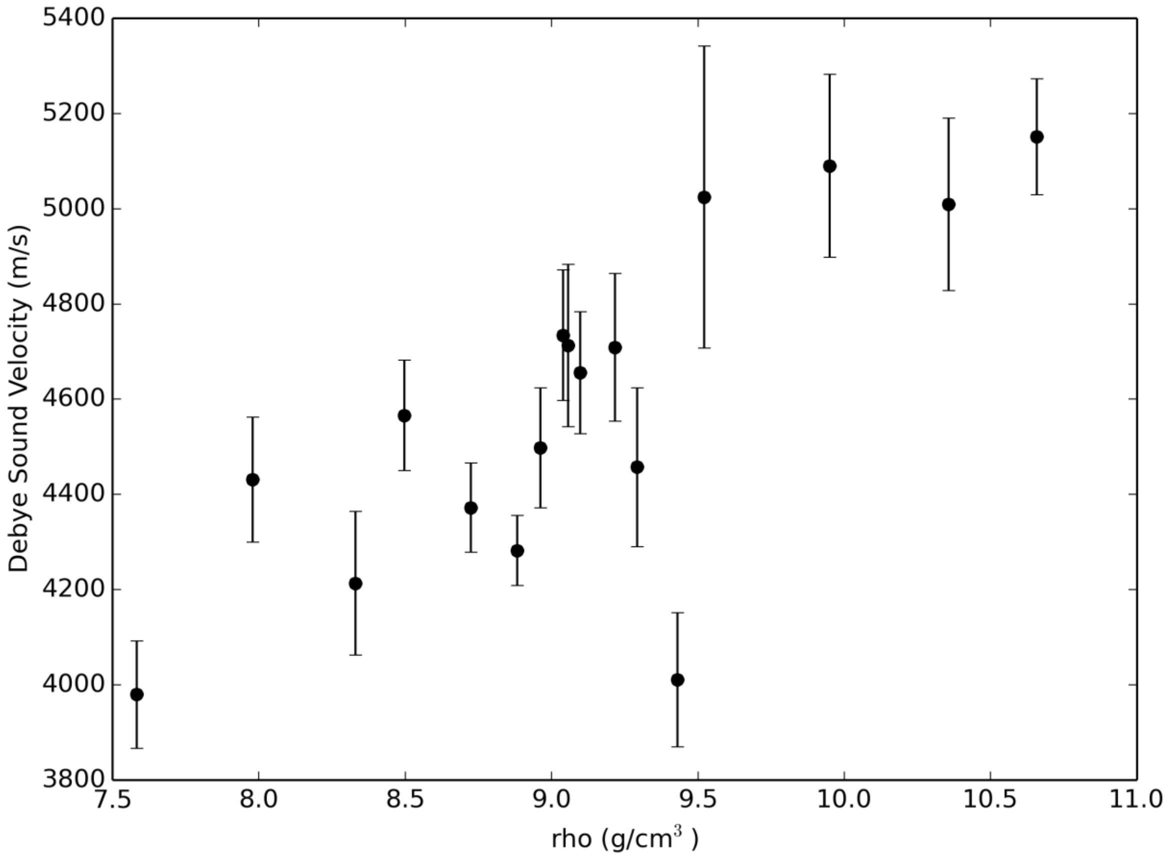

Figure S6 | Variation of Debye sound velocity v_d with density. Debye sound velocity increases linearly up to 9.3 (g/cm^3) but then decreases in the region of the para- to non-magnetic transition. Above 9.5 (g/cm^3) where the nonmagnetic phase is stable, v_D remains nearly constant with increasing density.

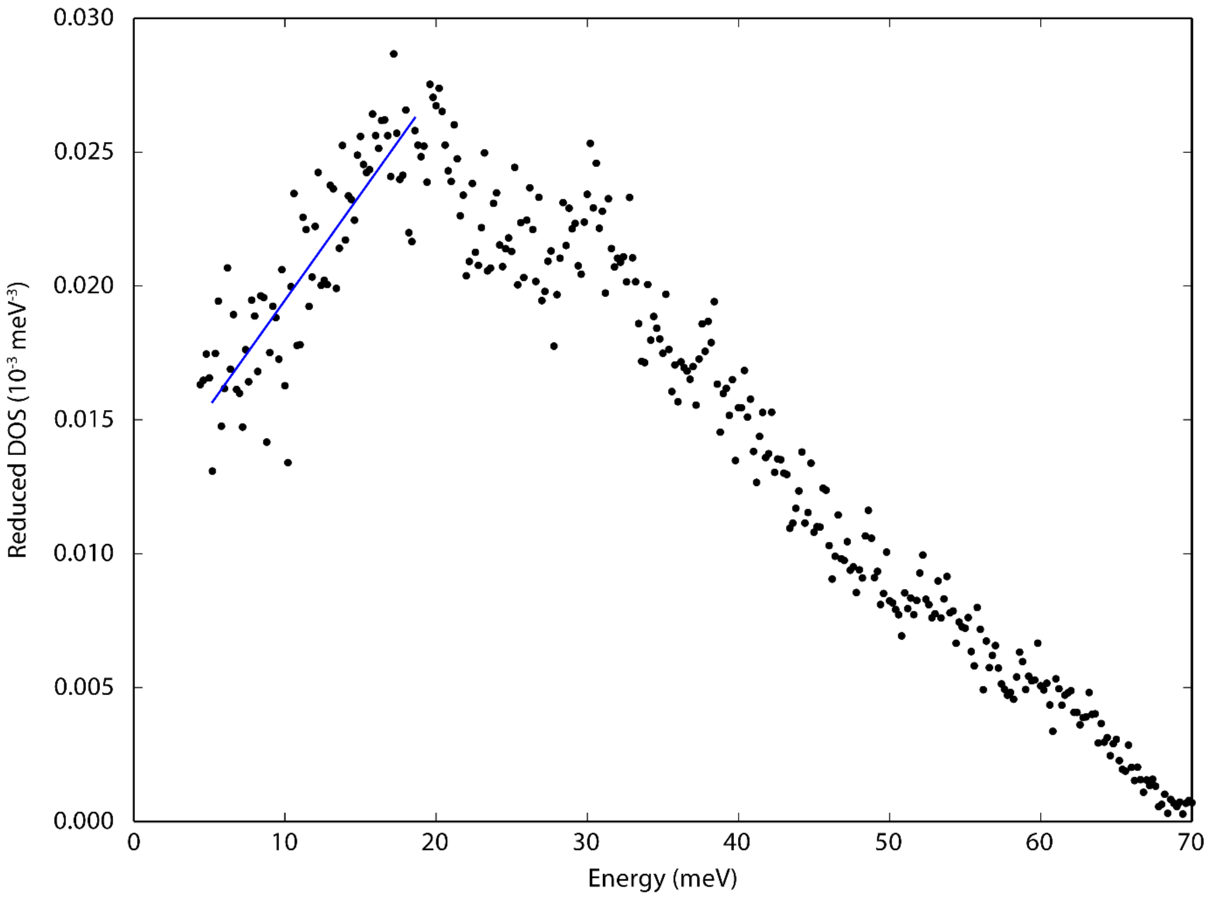

Figure S7 | Reduced density of phonon states *g(E)/E²* of o-Fe_7C_3 at 158 GPa. The blue line is a linear fit to the low energy region which is used in the extrapolation to 0 meV to extract v_D.

Extended data tables

Table S1 | X-ray experiment details and crystallographic parameters of o-Fe_7C_3 at ambient conditions

Empirical formula	Fe_7C_3
Formula weight (g/mol)	426.98
Temperature (K)	296(2)
Wavelength (Å)	0.7107
Crystal system	Orthorhombic
Space group	*Pbca*
a (Å)	11.9747(4)
b (Å)	4.5202(2)
c (Å)	13.7572(6)
V (Å^3)	744.65(5)
Z	8
Calculated density (g/cm^3)	7.617
Linear absorption coefficient (mm^{-1})	26.278
F(000)	1600
Crystal size (mm^3)	0.1503 x 0.0885 x 0.0146
Theta range for data collection (deg.)	2.96 to 34.27
Completeness to theta = 25.00°	99.7 %
Index ranges	$-18 < h < 18$, $-7 < k < 6$, $-17 < l < 21$
Reflections collected	4641
Independent reflections / R_{int}	1473 / 0.0353
Max. and min. transmission	0.682 and 0.206
Refinement method	Full matrix least squares on F^2
Data / restraints / parameters	1473 / 0 / 91
Goodness of fit on F^2	1.033
Final R indices [$I > 2\sigma(I)$]	$R_1 = 0.0359$, $wR_2 = 0.0823$
R indices (all data)	$R_1 = 0.0542$, $wR_2 = 0.0929$
Largest diff. peak and hole (e / Å^3)	2.022 and -1.477

Table S2. Synthesis conditions for o-Fe_7C_3 at different experimental conditions.

N	Type of experiment	Temperature, K	Pressure, GPa	Method of o-Fe_7C_3 identification
1	Multi-anvil apparatus, synthesis	1673(50)	7.0(5)	Single crystal diffraction; TEM
2	Multi-anvil apparatus, synthesis	1473(50)	12.0(5)	Single crystal diffraction; TEM
3	Multi-anvil apparatus, synthesis	1973(50)	15.0(5)	Single crystal diffraction
4	LH DAC**, in-house	2550(100)	48(2)	Synchrotron PXRD***
5	LH DAC, in-house	2800(100)	77(2)	Synchrotron PXRD
6	LH DAC, in-house	2750(100)	85(3)	Synchrotron PXRD
7	LH DAC, IDD-13	2900(100)	57(1)	Synchrotron PXRD
8	LH DAC, IDD-13	3100(100)	88(2)	Synchrotron PXRD
9	LH DAC, in-house	>3500	180(5)	TEM
10	LH DAC, in-house	>3700	205(10)	Synchrotron PXRD

*Samples were recovered at ambient conditions
**LH DAC – double-side laser-heated diamond anvil cell
***PXRD – powder X-ray diffraction

Table S3 | Interatomic distances (in Å) in CFe_6 trigonal prisms in the o-Fe_7C_3 crystal structure at ambient conditions

Prism 1		Prism 2		Prism 3	
C1–Fe1	1.984(5)	C2–Fe2	1.979(5)	C3–Fe3	1.964(5)
C1–Fe4	2.010(5)	C2–Fe4#3	1.997(5)	C3–Fe4#5	1.984(5)
C1–Fe1#1	2.014(5)	C2–Fe3#1	2.006(5)	C3–Fe3#1	2.025(5)
C1–Fe5#2	2.032(5)	C2–Fe5#1	2.038(5)	C3–Fe6#1	2.038(5)
C1–Fe7#1	2.033(5)	C2–Fe1#1	2.047(5)	C3–Fe7#6	2.043(5)
C1–Fe2#1	2.036(5)	C2–Fe6#4	2.057(5)	C3–Fe2#1	2.049(5)
Triangular bases:		*Triangular bases:*		*Triangular bases:*	
Fe1#1–Fe2#1	2.5532(8)	Fe1#1–Fe3#1	2.5261(8)	Fe2#1–Fe3#1	2.5453(8)
Fe1–Fe2#1	2.6776(8)	Fe1#1–Fe2	2.6782(8)	Fe2#1–Fe3	2.6608(8)
Fe1–Fe1#1	2.7208(8)	Fe2–Fe3#1	2.7406(8)	Fe3–Fe3#1	2.6901(8)
Fe5#2–Fe7#1	2.526(1)	Fe5#1–Fe6#4	2.5292(8)	Fe6#1–Fe7#6	2.547(1)
Fe4–Fe5#2	2.6072(8)	Fe4#3–Fe5#1	2.6072(8)	Fe4#5–Fe7#6	2.6851(9)
Fe4–Fe7#1	2.7414(9)	Fe4#3–Fe6#4	2.7393(8)	Fe4#5– Fe6#1	2.6722(8)
Lateral faces:		*Lateral faces:*		*Lateral faces:*	
Fe1–Fe4	2.6266(8)	Fe1#1–Fe5#1	2.6239(9)	Fe2#1– Fe6#1	2.6198(8)
Fe2#1–Fe5#2	2.6358(8)	Fe2–Fe4#3	2.6334(9)	Fe3#1–Fe7#6	2.6281(8)
Fe1#1-Fe7#1	2.6592(8)	Fe3#1–Fe6#4	2.6809(9)	Fe3–Fe4#5	2.6741(8)

Symmetry transformations used to generate equivalent atoms:

#1 ½ – x, ½ + y, z

#2 1 – x, ½ + y, ½ – z

#3 – ½ + x, y, ½ – z

#4 – x, 1 – y, 1 – z

#5 x, ½ – y, ½ + z

#6 ½ – x, 1– y, ½ + z

Table S4 | Lattice parameters, number of independent reflections N_{refl} and R1 factor derived from high-pressure single crystal X-ray diffraction measurements.

			Lattice Parameters			
P (GPa)	**a (Å)**	**b (Å)**	**c (Å)**	**V (Å³)**	**N_{refl}**	**R1 (%)**
3.92(5)	11.9050(2)	4.4883(1)	13.705(3)	732.30(16)	341	2.78
6.55(5)	11.8691(3)	4.4668(2)	13.646(4)	723.5(2)	313	3.63
11.1(1)	11.8021(3)	4.4262(2)	13.567(4)	708.7(2)	313	2.07
13.4(1)	11.7674(3)	4.4061(2)	13.535(4)	701.8(2)	309	2.15
16.95(5)	11.7183(6)	4.3766(3)	13.485(8)	691.6(4)	319	3.13
20.5(1)	11.644(3)	4.3510(3)	13.434(2)	680.6(2)	253	4.26
22.2(1)	11.6483(4)	4.3414(2)	13.420(6)	678.6(3)	299	3.82
27.3(1)	11.5903(4)	4.3132(2)	13.347(6)	667.2(3)	299	5.42
34.2(1)	11.5119(5)	4.2766(3)	13.274(7)	653.5(3)	284	8.54
46.0(3)	11.403(3)	4.2300(3)	13.173(2)	635.4(2)	230	7.94
61.9(1)	11.252(3)	4.1721(3)	13.046(2)	612.44(19)	222	7.8
83.2(2)	11.103(3)	4.1110(3)	12.894(2)	588.54(19)	218	7.17
84.0(2)	11.096(3)	4.1156(3)	12.885(2)	588.42(19)	219	8.07
101.2(1)	10.959(5)	4.0476(6)	12.731(4)	564.7(3)	212	10.83
101.0(1)	10.959(5)	4.0587(6)	12.752(3)	567.2(3)	213	8.75
110.95(5)	10.944(6)	4.0415(6)	12.729(4)	563.0(4)	210	9.09
111.7(1)	10.947(6)	4.0478(8)	12.716(5)	563.5(4)	216	6.83
124.0(0)	10.899(4)	4.0191(4)	12.658(3)	554.5(2)	325	7.59
125.2(1)	10.867(7)	4.0218(7)	12.662(4)	553.4(4)	307	7.89
134.2(2)	10.864(4)	3.9993(4)	12.602(3)	547.5(2)	311	7.56
134.1(2)	10.835(4)	3.9942(5)	12.586(2)	544.7(2)	319	8.52
139.8(1)	10.806(4)	3.9857(4)	12.562(3)	541.0(2)	319	8.16
140.3(2)	10.807(3)	3.985	12.568(2)	541.27(17)	320	7.46
151.6(2)	10.787(3)	3.9597(3)	12.486(2)	533.32(18)	298	7.27
151.6(2)	10.742(3)	3.9526(4)	12.482(2)	529.97(18)	310	8.53
158.0(1)	10.733(4)	3.9540(3)	12.493(2)	530.2(2)	294	7.91
157.9(2)	10.735(3)	3.9523(3)	12.4834(19)	529.64(17)	311	7.85

Table S5 | Fractional atomic positions for the o-Fe_7C_3 structure derived from high-pressure single crystal X-ray diffraction data.

P (GPa)		**3.92(5)**	**6.55(5)**	**11.1(1)**	**13.4(1)**	**16.95(5)**	**20.5(1)**
C1	x	0.8400(6)	0.8412(7)	0.8413(5)	0.8412(5)	0.8420(7)	0.8413(18)
	y	0.4646(15)	0.4661(18)	0.4651(12)	0.4666(12)	0.4698(17)	0.464(3)
	z	0.7666(13)	0.771(2)	0.7703(12)	0.7700(13)	0.7678(18)	0.7668(12)
	Uint	0.8400(6)	0.8412(7)	0.8413(5)	0.8412(5)	0.8420(7)	0.8413(18)
C2	x	0.5608(6)	0.5602(6)	0.5606(4)	0.5607(4)	0.5609(6)	0.5633(19)
	y	0.4652(13)	0.4620(17)	0.4651(11)	0.4646(11)	0.4692(17)	0.461(3)
	z	0.6204(12)	0.6232(18)	0.6224(12)	0.6237(12)	0.6206(18)	0.6189(10)
	Uint	0.5608(6)	0.5602(6)	0.5606(4)	0.5607(4)	0.5609(6)	0.5633(19)
C3	x	0.8438(6)	0.8439(7)	0.8424(5)	0.8431(5)	0.8427(7)	0.8455(19)
	y	0.4693(14)	0.4689(19)	0.4690(13)	0.4672(12)	0.4691(18)	0.471(3)
	z	0.4842(12)	0.4819(18)	0.4836(11)	0.4845(12)	0.4881(19)	0.4841(12)
	Uint	0.8438(6)	0.8439(7)	0.8424(5)	0.8431(5)	0.8427(7)	0.8455(19)
Fe1	x	0.81305(7)	0.81310(9)	0.81307(6)	0.81302(6)	0.81291(9)	0.8128(2)
	y	0.06027(16)	0.0591(2)	0.05772(15)	0.05684(17)	0.0559(2)	0.0561(4)
	z	0.71646(18)	0.7161(3)	0.71654(18)	0.71651(19)	0.7165(3)	0.71646(16)
	Uint	0.81305(7)	0.81310(9)	0.81307(6)	0.81302(6)	0.81291(9)	0.8128(2)
Fe2	x	0.62721(8)	0.62715(10)	0.62697(6)	0.62706(6)	0.62689(9)	0.6267(3)
	y	0.06041(18)	0.0594(2)	0.05812(15)	0.05683(15)	0.0562(2)	0.0560(4)
	z	0.62559(18)	0.6250(3)	0.62501(18)	0.62538(18)	0.6253(3)	0.62536(15)
	Uint	0.62721(8)	0.62715(10)	0.62697(6)	0.62706(6)	0.62689(9)	0.6267(3)
Fe3	x	0.81090(8)	0.81087(10)	0.81094(6)	0.81109(6)	0.81106(10)	0.8111(2)
	y	0.06989(17)	0.0689(2)	0.06737(16)	0.06642(16)	0.0650(2)	0.0646(4)
	z	0.53244(19)	0.5331(3)	0.53271(19)	0.53254(19)	0.5325(3)	0.53234(17)
	Uint	0.81090(8)	0.81087(10)	0.81094(6)	0.81109(6)	0.81106(10)	0.8111(2)
Fe4	x	0.91790(8)	0.91785(10)	0.91784(7)	0.91793(6)	0.91790(10)	0.9172(3)
	y	0.24093(15)	0.2410(2)	0.24106(13)	0.24085(14)	0.2409(2)	0.2409(3)
	z	0.8731(2)	0.8736(2)	0.8732(2)	0.8732(3)	0.8735(3)	0.87325(17)
	Uint	0.91790(8)	0.91785(10)	0.91784(7)	0.91793(6)	0.91790(10)	0.9172(3)
Fe5	x	1.02329(8)	1.02322(9)	1.02315(7)	1.02298(7)	1.02294(10)	1.0228(2)
	y	0.22815(18)	0.2285(2)	0.22954(16)	0.22995(16)	0.2308(2)	0.2324(4)
	z	0.71516(19)	0.7148(3)	0.7155(2)	0.7156(2)	0.7154(3)	0.71593(15)
	Uint	1.02329(8)	1.02322(9)	1.02315(7)	1.02298(7)	1.02294(10)	1.0228(2)
Fe6	x	0.52438(9)	0.52416(9)	0.52385(7)	0.52358(8)	0.52335(11)	0.5230(3)
	y	0.25023(15)	0.2503(2)	0.25042(15)	0.24990(15)	0.2499(2)	0.2502(3)
	z	0.4693(2)	0.4685(3)	0.4685(2)	0.4686(2)	0.4685(3)	0.46851(16)
	Uint	0.52438(9)	0.52416(9)	0.52385(7)	0.52358(8)	0.52335(11)	0.5230(3)
Fe7	x	0.70736(9)	0.70744(11)	0.70738(6)	0.70731(6)	0.70748(9)	0.7081(3)
	y	0.24818(16)	0.2481(2)	0.24793(14)	0.24775(14)	0.2477(2)	0.2480(3)
	z	0.87474(17)	0.8749(3)	0.8751(2)	0.8750(2)	0.8748(3)	0.87499(14)
	Uint	0.70736(9)	0.70744(11)	0.70738(6)	0.70731(6)	0.70748(9)	0.7081(3)

Table S5 | Continued.

P (GPa)		22.2(1)	27.3(1)	34.2(1)	46.0(3)	61.9(1)	83.2(2)
C1	x	0.8420(8)	0.8415(12)	0.840(2)	0.835(3)	0.835(3)	0.846(3)
	y	0.467(2)	0.468(3)	0.467(5)	0.462(5)	0.465(6)	0.456(5)
	z	0.769(2)	0.772(3)	0.774(6)	0.764(2)	0.766(2)	0.7696(16)
	Uint	0.8420(8)	0.8415(12)	0.840(2)	0.835(3)	0.835(3)	0.846(3)
C2	x	0.5607(7)	0.5613(10)	0.5609(16)	0.563(3)	0.568(3)	0.572(4)
	y	0.467(2)	0.464(2)	0.469(4)	0.464(4)	0.464(5)	0.461(5)
	z	0.6219(18)	0.624(3)	0.623(4)	0.6193(12)	0.6187(15)	0.6148(16)
	Uint	0.5607(7)	0.5613(10)	0.5609(16)	0.563(3)	0.568(3)	0.572(4)
C3	x	0.8435(8)	0.8428(12)	0.8428(19)	0.841(3)	0.841(3)	0.850(3)
	y	0.468(2)	0.466(3)	0.485(5)	0.486(5)	0.487(6)	0.477(5)
	z	0.4843(18)	0.486(3)	0.480(4)	0.483(2)	0.481(2)	0.4912(18)
	Uint	0.8435(8)	0.8428(12)	0.8428(19)	0.841(3)	0.841(3)	0.850(3)
Fe1	x	0.81302(9)	0.81269(14)	0.8123(2)	0.8122(4)	0.8126(4)	0.8127(5)
	y	0.0552(3)	0.0542(3)	0.0530(6)	0.0517(7)	0.0507(8)	0.0487(10)
	z	0.7166(3)	0.7169(4)	0.7164(7)	0.7169(3)	0.7169(3)	0.7161(3)
	Uint	0.81302(9)	0.81269(14)	0.8123(2)	0.8122(4)	0.8126(4)	0.8127(5)
Fe2	x	0.62694(11)	0.62687(15)	0.6269(2)	0.6265(5)	0.6271(5)	0.6249(6)
	y	0.0548(3)	0.0533(4)	0.0517(6)	0.0527(7)	0.0508(7)	0.0475(9)
	z	0.6249(3)	0.6250(4)	0.6251(7)	0.6252(2)	0.6250(3)	0.6242(3)
	Uint	0.62694(11)	0.62687(15)	0.6269(2)	0.6265(5)	0.6271(5)	0.6249(6)
Fe3	x	0.81113(11)	0.81117(16)	0.8110(3)	0.8113(3)	0.8112(3)	0.8114(4)
	y	0.0637(3)	0.0622(3)	0.0610(6)	0.0575(6)	0.0554(7)	0.0521(10)
	z	0.5325(3)	0.5320(4)	0.5312(7)	0.5321(3)	0.5324(3)	0.5315(3)
	Uint	0.81113(11)	0.81117(16)	0.8110(3)	0.8113(3)	0.8112(3)	0.8114(4)
Fe4	x	0.91771(13)	0.91767(18)	0.9172(3)	0.9151(6)	0.9180(7)	0.9188(9)
	y	0.2407(2)	0.2411(3)	0.2413(5)	0.2398(6)	0.2404(6)	0.2408(8)
	z	0.8734(3)	0.8730(4)	0.8722(7)	0.87338(16)	0.8737(3)	0.8751(2)
	Uint	0.91771(13)	0.91767(18)	0.9172(3)	0.9151(6)	0.9180(7)	0.9188(9)
Fe5	x	1.02297(10)	1.02293(15)	1.0231(3)	1.0218(4)	1.0224(5)	1.0204(5)
	y	0.2328(3)	0.2338(3)	0.2353(6)	0.2366(6)	0.2383(6)	0.2409(7)
	z	0.7158(3)	0.7166(4)	0.7170(7)	0.7166(3)	0.7168(3)	0.7177(3)
	Uint	1.02297(10)	1.02293(15)	1.0231(3)	1.0218(4)	1.0224(5)	1.0204(5)
Fe6	x	0.52326(10)	0.52309(15)	0.5231(3)	0.5209(4)	0.5214(5)	0.5209(5)
	y	0.2493(2)	0.2491(3)	0.2500(5)	0.2504(5)	0.2507(6)	0.2503(8)
	z	0.4683(3)	0.4679(4)	0.4684(7)	0.4684(3)	0.4688(3)	0.4674(3)
	Uint	0.52326(10)	0.52309(15)	0.5231(3)	0.5209(4)	0.5214(5)	0.5209(5)
Fe7	x	0.70750(12)	0.70745(18)	0.7078(3)	0.7086(6)	0.7068(8)	0.7055(7)
	y	0.2477(3)	0.2478(3)	0.2479(6)	0.2478(6)	0.2474(5)	0.2473(7)
	z	0.8747(2)	0.8748(4)	0.8751(6)	0.87529(15)	0.8754(2)	0.8761(2)
	Uint	0.70750(12)	0.70745(18)	0.7078(3)	0.7086(6)	0.7068(8)	0.7055(7)

Table S5 | Continued.

P (GPa)		84.0(2)	101.2(1)	101.0(1)	110.95(5)	111.7(1)
C1	x	0.841(3)	0.833(2)	0.839(3)	0.835(3)	0.844(3)
	y	0.466(4)	0.471(5)	0.464(5)	0.470(5)	0.461(5)
	z	0.7718(18)	0.7623(17)	0.7683(18)	0.7626(19)	0.770(2)
	Uint	0.841(3)	0.833(2)	0.839(3)	0.835(3)	0.844(3)
C2	x	0.572(3)	0.564(3)	0.571(2)	0.570(4)	0.565(3)
	y	0.465(4)	0.468(4)	0.463(3)	0.466(4)	0.467(3)
	z	0.6214(13)	0.6199(14)	0.6223(10)	0.6192(13)	0.6232(11)
	Uint	0.572(3)	0.564(3)	0.571(2)	0.570(4)	0.565(3)
C3	x	0.841(3)	0.833(3)	0.843(3)	0.839(3)	0.836(2)
	y	0.481(4)	0.481(5)	0.479(4)	0.479(4)	0.482(4)
	z	0.4846(18)	0.4835(18)	0.4848(18)	0.4846(18)	0.4820(17)
	Uint	0.841(3)	0.833(3)	0.843(3)	0.839(3)	0.836(2)
Fe1	x	0.8122(4)	0.8120(5)	0.8121(3)	0.8123(5)	0.8126(3)
	y	0.0496(8)	0.0480(9)	0.0486(7)	0.0471(8)	0.0478(7)
	z	0.7166(3)	0.7175(3)	0.7165(3)	0.7174(3)	0.7166(2)
	Uint	0.8122(4)	0.8120(5)	0.8121(3)	0.8123(5)	0.8126(3)
Fe2	x	0.6271(4)	0.6255(6)	0.6266(4)	0.6257(5)	0.6267(4)
	y	0.0477(6)	0.0467(8)	0.0465(6)	0.0456(8)	0.0457(6)
	z	0.6253(2)	0.6252(3)	0.62539(19)	0.6254(2)	0.62519(18)
	Uint	0.6271(4)	0.6255(6)	0.6266(4)	0.6257(5)	0.6267(4)
Fe3	x	0.8113(3)	0.8111(4)	0.8113(3)	0.8115(4)	0.8111(3)
	y	0.0544(8)	0.0516(9)	0.0522(7)	0.0506(8)	0.0510(6)
	z	0.5323(3)	0.5316(3)	0.5322(2)	0.5322(3)	0.5322(2)
	Uint	0.8113(3)	0.8111(4)	0.8113(3)	0.8115(4)	0.8111(3)
Fe4	x	0.9173(5)	0.9181(10)	0.9172(5)	0.9185(8)	0.9175(6)
	y	0.2408(7)	0.2405(7)	0.2409(6)	0.2411(7)	0.2398(6)
	z	0.87309(17)	0.8735(2)	0.87322(15)	0.87330(19)	0.87323(16)
	Uint	0.9173(5)	0.9181(10)	0.9172(5)	0.9185(8)	0.9175(6)
Fe5	x	1.0212(4)	1.0208(5)	1.0208(4)	1.0208(5)	1.0203(3)
	y	0.2420(6)	0.2417(7)	0.2434(6)	0.2434(7)	0.2433(5)
	z	0.7176(2)	0.7168(3)	0.7173(2)	0.7170(3)	0.7178(2)
	Uint	1.0212(4)	1.0208(5)	1.0208(4)	1.0208(5)	1.0203(3)
Fe6	x	0.5207(4)	0.5202(5)	0.5203(4)	0.5200(5)	0.5202(3)
	y	0.2499(5)	0.2490(6)	0.2500(5)	0.2489(7)	0.2501(5)
	z	0.4688(2)	0.4685(3)	0.4687(2)	0.4687(3)	0.4688(2)
	Uint	0.5207(4)	0.5202(5)	0.5203(4)	0.5200(5)	0.5202(3)
Fe7	x	0.7068(4)	0.7064(7)	0.7069(4)	0.7057(6)	0.7066(4)
	y	0.2476(6)	0.2468(7)	0.2472(6)	0.2464(6)	0.2470(5)
	z	0.87497(19)	0.8758(2)	0.87522(19)	0.87556(18)	0.87531(19)
	Uint	0.7068(4)	0.7064(7)	0.7069(4)	0.7057(6)	0.7066(4)

Table S5 | Continued.

P (GPa)		124.0(0)	125.2(1)	134.2(2)	134.1(2)	139.8(1)
C1	x	0.8446(18)	0.8415(19)	0.844(2)	0.843(2)	0.843(2)
	y	0.465(3)	0.470(4)	0.464(4)	0.464(4)	0.467(4)
	z	0.7673(11)	0.7659(13)	0.7651(15)	0.7673(15)	0.7677(14)
	Uint	0.8446(18)	0.8415(19)	0.844(2)	0.843(2)	0.843(2)
C2	x	0.569(2)	0.571(2)	0.573(2)	0.571(3)	0.565(3)
	y	0.466(3)	0.461(3)	0.463(3)	0.457(4)	0.466(3)
	z	0.6227(8)	0.6221(10)	0.6204(11)	0.6222(12)	0.6235(13)
	Uint	0.569(2)	0.571(2)	0.573(2)	0.571(3)	0.565(3)
C3	x	0.8463(16)	0.8469(17)	0.8475(19)	0.844(2)	0.845(2)
	y	0.470(2)	0.473(3)	0.470(3)	0.471(3)	0.482(4)
	z	0.4831(10)	0.4839(10)	0.4844(11)	0.4833(13)	0.4818(12)
	Uint	0.8463(16)	0.8469(17)	0.8475(19)	0.844(2)	0.845(2)
Fe1	x	0.8127(3)	0.8130(3)	0.8125(3)	0.8130(3)	0.8130(3)
	y	0.0467(5)	0.0462(5)	0.0467(6)	0.0455(6)	0.0463(6)
	z	0.71700(17)	0.71648(18)	0.71664(19)	0.71625(19)	0.7169(2)
	Uint	0.8127(3)	0.8130(3)	0.8125(3)	0.8130(3)	0.8130(3)
Fe2	x	0.6277(3)	0.6267(3)	0.6274(3)	0.6262(4)	0.6277(3)
	y	0.0450(4)	0.0456(5)	0.0452(5)	0.0446(6)	0.0452(5)
	z	0.62517(14)	0.62560(15)	0.62531(16)	0.62520(17)	0.62522(17)
	Uint	0.6277(3)	0.6267(3)	0.6274(3)	0.6262(4)	0.6277(3)
Fe3	x	0.8122(2)	0.8124(3)	0.8125(2)	0.8125(3)	0.8116(3)
	y	0.0496(5)	0.0492(5)	0.0494(5)	0.0487(6)	0.0494(5)
	z	0.53209(16)	0.53270(17)	0.5325(2)	0.53262(18)	0.5324(2)
	Uint	0.8122(2)	0.8124(3)	0.8125(2)	0.8125(3)	0.8116(3)
Fe4	x	0.9173(4)	0.9184(4)	0.9170(4)	0.9180(4)	0.9178(4)
	y	0.2404(4)	0.2412(5)	0.2408(4)	0.2402(5)	0.2396(5)
	z	0.87300(14)	0.87301(12)	0.87319(17)	0.87313(13)	0.8734(2)
	Uint	0.9173(4)	0.9184(4)	0.9170(4)	0.9180(4)	0.9178(4)
Fe5	x	1.0209(3)	1.0212(3)	1.0207(3)	1.0207(3)	1.0204(3)
	y	0.2446(4)	0.2464(5)	0.2451(5)	0.2462(5)	0.2458(5)
	z	0.71695(16)	0.71672(16)	0.71708(18)	0.71673(18)	0.71694(18)
	Uint	1.0209(3)	1.0212(3)	1.0207(3)	1.0207(3)	1.0204(3)
Fe6	x	0.5207(3)	0.5206(3)	0.5205(3)	0.5204(3)	0.5204(3)
	y	0.2495(4)	0.2502(4)	0.2491(4)	0.2502(5)	0.2503(4)
	z	0.46917(16)	0.46853(16)	0.46928(17)	0.46858(18)	0.46922(18)
	Uint	0.5207(3)	0.5206(3)	0.5205(3)	0.5204(3)	0.5204(3)
Fe7	x	0.7068(3)	0.7067(3)	0.7069(3)	0.7064(3)	0.7069(3)
	y	0.2468(4)	0.2479(5)	0.2461(4)	0.2463(5)	0.2470(5)
	z	0.87530(16)	0.87543(11)	0.8753(2)	0.87531(12)	0.8750(2)
	Uint	0.7068(3)	0.7067(3)	0.7069(3)	0.7064(3)	0.7069(3)

Table S5 |Continued.

P (GPa)		151.6(2)	158.0(1)	157.9(2)
C1	x	0.839(2)	0.843(3)	0.841(2)
	y	0.467(4)	0.471(4)	0.468(4)
	z	0.7663(15)	0.7683(16)	0.7662(17)
	Uint	0.839(2)	0.843(3)	0.841(2)
C2	x	0.566(3)	0.576(3)	0.568(4)
	y	0.452(4)	0.469(3)	0.460(4)
	z	0.6217(12)	0.6214(13)	0.6221(13)
	Uint	0.566(3)	0.576(3)	0.568(4)
C3	x	0.847(2)	0.845(2)	0.848(2)
	y	0.472(3)	0.475(3)	0.472(3)
	z	0.4803(13)	0.4854(13)	0.4838(14)
	Uint	0.847(2)	0.845(2)	0.848(2)
Fe1	x	0.8126(3)	0.8124(3)	0.8126(3)
	y	0.0445(6)	0.0450(6)	0.0442(6)
	z	0.71625(18)	0.7166(2)	0.71656(19)
	Uint	0.8126(3)	0.8124(3)	0.8126(3)
Fe2	x	0.6269(4)	0.6274(4)	0.6266(4)
	y	0.0438(5)	0.0448(5)	0.0436(5)
	z	0.62527(16)	0.62537(19)	0.62527(16)
	Uint	0.6269(4)	0.6274(4)	0.6266(4)
Fe3	x	0.8123(3)	0.8118(3)	0.8127(3)
	y	0.0464(6)	0.0483(5)	0.0458(5)
	z	0.53258(18)	0.5325(2)	0.53258(18)
	Uint	0.8123(3)	0.8118(3)	0.8127(3)
Fe4	x	0.9178(4)	0.9170(4)	0.9181(5)
	y	0.2398(5)	0.2395(5)	0.2403(5)
	z	0.87316(13)	0.8733(2)	0.87316(14)
	Uint	0.9178(4)	0.9170(4)	0.9181(5)
Fe5	x	1.0201(3)	1.0203(3)	1.0204(3)
	y	0.2454(6)	0.2458(5)	0.2464(6)
	z	0.71647(18)	0.7177(2)	0.71696(19)
	Uint	1.0201(3)	1.0203(3)	1.0204(3)
Fe6	x	0.5197(3)	0.5197(3)	0.5201(3)
	y	0.2503(5)	0.2505(4)	0.2498(4)
	z	0.46838(17)	0.4692(2)	0.46894(18)
	Uint	0.5197(3)	0.5197(3)	0.5201(3)
Fe7	x	0.7064(3)	0.7062(3)	0.7065(3)
	y	0.2463(5)	0.2463(5)	0.2459(5)
	z	0.87555(13)	0.8754(2)	0.87542(13)
	Uint	0.7064(3)	0.7062(3)	0.7065(3)

Table S6 | Isothermal bulk modulus K_T, shear modulus G, Debye velocity v_D, bulk velocity v_φ, compressional wave velocity v_P, shear wave velocity v_S and Poisson's ratio ν at 300 K and 1800 K for o-Fe_7C_3. Errors in pressure were estimated from the difference in ruby fluorescence measurements before and after each NIS data collection. Densities were calculated from the SXRD equation-of-state parameters.

P (GPa)	ρ (g/cm^3)	K_T (GPa)	G (GPa)	v_D (m/s)	v_φ (m/s)	v_P (m/s)	v_S (m/s)	ν
300 K								
0(0)	7.58(1)	168(5)	97(6)	3980(113)	4709(64)	6267(71)	3581(107)	0.26(2)
10(0)	7.98(1)	226(5)	127(8)	4431(131)	5326(61)	7038(67)	3985(125)	0.26(3)
21(0)	8.33(2)	286(6)	118(9)	4213(151)	5863(61)	7297(63)	3763(144)	0.32(3)
27(0)	8.50(2)	318(6)	142(8)	4566(116)	6116(63)	7724(66)	4085(110)	0.31(2)
36(0)	8.72(2)	364(7)	132(6)	4372(94)	6460(62)	7871(63)	3895(89)	0.34(2)
42.8(8)	8.88(3)	398(8)	129(5)	4282(74)	6697(72)	8011(72)	3806(70)	0.35(2)
46(0)	8.96(2)	417(8)	144(9)	4498(126)	6817(62)	8236(63)	4003(120)	0.35(3)
50(0)	9.04(2)	434(8)	161(10)	4734(137)	6931(63)	8472(65)	4219(131)	0.34(3)
51(0)	9.06(2)	439(8)	160(12)	4713(171)	6959(63)	8482(64)	4199(162)	0.34(4)
53(2)	9.10(4)	448(11)	156(9)	4655(128)	7020(86)	8496(87)	4144(122)	0.34(3)
59.0(5)	9.22(2)	478(9)	162(11)	4709(155)	7198(66)	8672(67)	4189(148)	0.35(3)
63(0)	9.29(2)	497(9)	145(12)	4457(167)	7311(64)	8620(64)	3955(159)	0.37(4)
70.5(5)	9.43(2)	532(9)	118(9)	4011(141)	7514(67)	8557(66)	3545(134)	0.40(4)
75.8(3)	9.52(2)	557(10)	190(26)	5025(317)	7652(67)	9230(68)	4471(302)	0.35(6)
103(3)	9.95(5)	683(19)	203(17)	5090(192)	8287(115)	9793(115)	4518(183)	0.36(4)
133(3)	10.36(5)	818(19)	204(16)	5009(181)	8889(104)	10258(103)	4434(173)	0.39(4)
158(5)	10.66(6)	929(27)	221(11)	5151(122)	9334(139)	10715(136)	4557(116)	0.39(3)
1800(200) K								
50(1)	9.04(3)	434(9)	154(11)	4630(155)	6928(76)	8406(77)	4123(148)	0.34(3)
62(1)	9.27(3)	492(10)	150(8)	4532(115)	7283(74)	8639(74)	4025(109)	0.36(3)
63(2)	9.29(4)	497(13)	98(12)	3680(207)	7311(96)	8217(94)	3247(197)	0.41(6)
85(2)	9.67(4)	600(14)	132(8)	4175(114)	7878(91)	8956(89)	3689(108)	0.40(3)